Time-division multiplexing of high-resolution TES X-ray microcalorimeters: Four pixels and beyond

W.B. Doriese, J.A. Beall, S. Deiker, W.D. Duncan, L. Ferreira, G.C. Hilton, K.D. Irwin, C.D. Reintsema, J.N. Ullom, L.R. Vale, and Y. Xu

National Institute of Standards and Technology
Mail Stop 814.03
325 Broadway
Boulder, CO 80305

Time-division multiplexing of high-resolution TES X-ray microcalorimeters: Four pixels and beyond

W. B. Doriese,[*] J. A. Beall, S. Deiker, W. D. Duncan, L. Ferreira, G. C. Hilton, K. D. Irwin, C. D. Reintsema, J. N. Ullom, L. R. Vale, and Y. Xu

National Institute of Standards and Technology

325 Broadway, MC 817.03

Boulder, CO 80305

(Dated: July 13, 2004)

Abstract

We present experimental results from a four-pixel array of transition-edge-sensor, X-ray microcalorimeters read out through a single amplifier channel via a time-division-SQUID multiplexer. We map the dependence of the X-ray energy resolution of the microcalorimeters on multiplexer timing parameters. We achieve multiplexed, four-pixel resolution of 6.94 ± 0.05 eV (FWHM) of the Mn $K\alpha$ complex near 5.9 keV, which is a degradation of only 0.44 eV from non-multiplexed operation. An analysis of straightforward upgrades to the multiplexer predicts that a linear array of 32 of these pixels could be multiplexed with a degradation in resolution of only 0.1 eV. These results are the first demonstration of a time-division multiplexer for X-ray detectors, and establish a clear path to the instrumentation of a kilopixel microcalorimeter array.

---

[*]doriese@boulder.nist.gov

Large arrays of transition-edge sensors (TESs) are planned for many applications, from astronomical cameras for the X-ray (Constellation-X, XEUS) and far-infrared to millimeter (SCUBA-2, ACT, APEX, SPT, SPIFI, SAFIRE) bands to X-ray materials analysis and γ-ray spectrometry of radioactive isotopes. The TES, a superconducting thin film that is electrically biased in the resistive transition between its normal and superconducting states, derives its sensitivity from its strong change in resistance when heated by photon absorption and from the low noise at typical operating temperatures of 100 mK. TESs are usually read out with multistage, superconducting-quantum-interference-device (SQUID) amplifiers, taking advantage of the low noise, low power dissipation, and low input impedance of SQUIDs.

The complexity inherent in instrumenting large arrays of TESs with individual SQUID amplifier channels has motivated the development of multiplexing schemes to read out arrays efficiently. Two classes of multiplexers are under development: time-division[1–3] and frequency-division[4–6]. A large, two-dimensional, time-division multiplexer array for submillimeter TES bolometers has been demonstrated[7]; however, arrays of X-ray microcalorimeters make far more stringent demands on the multiplexer speed and dynamic range.

In this letter, we describe the performance of a time-division multiplexer as it reads out four TES X-ray microcalorimeters through a single amplifier channel. The TESs are the center four of an 8×8-pixel array. Each 400 μm square sensor consists of a Mo-Cu bilayer (65 nm thick Mo, 175 nm Cu) with an absorber of 1500 nm Bi plus 500 nm Cu. Thermal isolation is provided by suspending each sensor on a 500 nm thick SiN_x membrane, with the bulk Si behind the pixel removed via a deep-reactive-ion-etch process. The four pixels have superconducting critical temperatures of 86.2±0.2 mK. An ^{55}Fe source within the cryostat provides X rays, which are collimated to a 200 μm square patch at the center of each detector; the resulting X-ray count rate is 2.8 Hz on each of the four pixels. A shutter allows the X rays to be blocked for I–V curve and noise spectrum acquisition. The thermal bath is cooled and regulated to 62 mK. The pixels are voltage biased to 30 % of the 21 mΩ normal-state resistance, are in a perpendicular magnetic field of 700 nT (7 mG), and have a transition sharpness of $\alpha = (T/R)(dR/dT)$ of 310 ± 30. The detectors' X-ray pulse responses have a rise time of $\tau_{rise} = 20$ μs (determined by the resistance of the TES and the inductance in its bias loop) and a fall time of $\tau_{fall} = 700$ μs (set by the detector's thermal time constant

2

and the strength of the electro-thermal feedback). The average pulse signal from a Mn $K\alpha$ X ray and the measured noise predict a best-possible spectral resolution of 6.2 eV (FWHM) at 5.9 keV; we consistently achieve resolution of 6.5 ± 0.15 eV in spectra of the Mn $K\alpha$ complex when measuring any of the four detectors with a non-multiplexed readout.

To read out the sensors, we use four elements of a NIST-developed, 1×32 SQUID multiplexer[2, 3]. In this architecture, each TES is inductively coupled to its own first-stage SQUID amplifier. An inductive summing coil carries the output signals from the first-stage SQUIDs to a common second-stage SQUID amplifier, located on the same chip. When in the superconducting (off) state, each first-stage SQUID contributes no signal and no noise. The first stage SQUIDs are sequentially biased, or addressed, into their resistive (on) state, so the signal from one pixel at a time is passed to the second stage amplifier. Finally, the output of the second-stage SQUID is routed to a series-array SQUID amplifier[8] and then to room-temperature electronics. The three-stage SQUID amplifier thus described is highly nonlinear; its transfer function, or V–Φ curve, is approximated by a sinusoid with a period of the magnetic flux quantum, Φ_0. To keep the amplifier chain stably in a linear portion of this curve, the multiplexer is run as a flux-locked loop. The series array output, or error signal (V_{ER}), is sampled by an analog-to-digital converter, and then a digitally-generated, proportional-integral, flux-feedback signal (V_{FB}) is applied inductively to the first stage SQUIDs in order to keep V_{ER} at a constant value.

Fig. 1 shows time streams of V_{ER} and V_{FB} for two multiplexed pixels. Synchronized electronics apply the address current to the first-stage-SQUID amplifier for pixel A, and simultaneously apply V_{FB} as calculated previously for the pixel. After waiting a time, t_{SET}, for the switching transient to settle, the electronics record V_{ER} (averaging over the sampling time, t_{SAM}), and calculate the appropriate feedback signal for the next visit to pixel A. Finally, pixel A's address bias and V_{FB} are turned off, pixel B's are turned on, and the sequence is repeated for pixel B. The frame time, defined as the time between visits to a pixel, is given by

$$t_{FR} = N_{MUX} \ (t_{SET} + t_{SAM}), \tag{1}$$

where N_{MUX} is the number of multiplexed pixels.

The energy resolution of our detectors is determined by measuring a spectrum of the Mn $K\alpha$ complex at 5.9 keV. V_{ER} and V_{FB} are recorded in a time stream for between 5000 and 10000 X-ray pulses per pixel, and are then de-multiplexed and triggered in software.
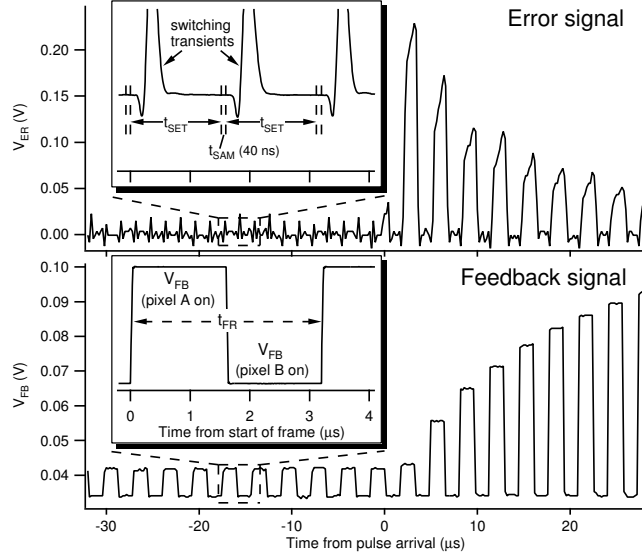
FIG. 1: Error and feedback signals vs. time for two multiplexed pixels, A and B. Pixel A shows the rising edge of a pulse from an X-ray impact at time 0. The feedback signal, V_{FB}, and the row address signal (not pictured) for pixel A are turned on at the beginning of the frame. After a settling time, t_{SET}, in this example 1.56 μs, the error signal, V_{ER}, is averaged over the sampling time ($t_{SAM} = 40$ ns), and then pixel A is turned off and B is turned on. Pixels A and B have different quiescent signal levels due to slight differences in the sensor critical temperatures and first-stage-SQUID operating conditions.

The current through the TES is calculated by $I_{TES} \propto V_{FB} + V_{ER}/m_{SQ}$, where m_{SQ} is the slope of the 3-stage SQUID V–Φ curve at the bias point. Pulse heights are calculated from the raw pulses via an optimal filter[e.g. 9], and the filtered, corrected pulse heights are histogrammed, mapped to X-ray energy using known line energies, and fit to the natural line widths[10] of the Mn $K\alpha$ complex to determine the FWHM energy resolution of the detector.

Our first experiment involves only two of the four detectors. We map the effects of the multiplexer timing, measuring energy resolution while holding fixed t_{SAM}, at 0.04 μs, and varying t_{SET}, and thus t_{FR} (see Eq. 1); the results of this two-pixel experiment are plotted in Fig. 2. For a variety of choices of t_{SET}, the multiplexer reads out the two pixels without significant resolution degradation. However, if the multiplexer is run either too quickly or too slowly, the energy resolution degrades and ultimately the multiplexer unlocks. As the multiplexer is run more slowly (larger t_{FR}) the signal for each pixel is not sampled as
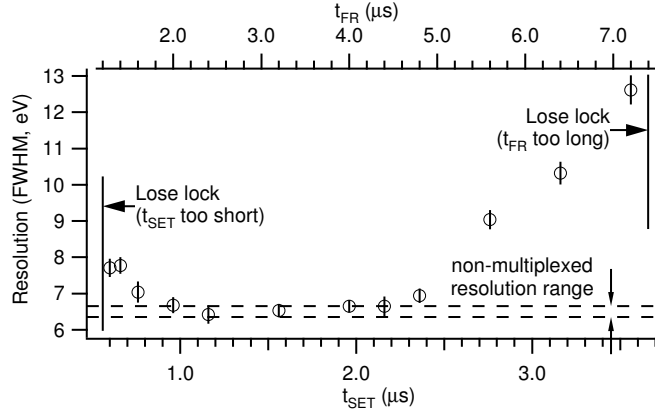
FIG. 2: Measured TES resolution vs. t_{SET} for two multiplexed pixels. The top axis gives t_{FR} as calculated using Eq. 1 with $t_{SAM} = 40$ ns. The poorer resolution to the left of the plot is due to t_{SET} being too short to allow switching transients to decay fully before sampling. The degradation to the right is due to taking too few samples on the pulse rise, where the signal changes the fastest. In either of the limits $t_{SET} \leq 0.56$ μs or $t_{FR} \geq 7.4$ μs, the multiplexer loses lock.

often, and V_{ER} grows large on the rising edge of a pulse, the fastest-changing part of the signal. The large and non-linear V_{ER} and slew-limited V_{FB} signals provide an increasingly unfaithful representation of the TES current, and the energy resolution degrades (henceforth referred to as the t_{FR} effect). In the extreme case, $t_{FR} \geq 7.4$ μs, or only 2.7 data samples in the pulse's τ_{rise}, the error signal wraps over the top of the SQUID V–Φ curve and the loop unlocks. At the other end of the timing scale, as the multiplexer is run more quickly, sampling during the switching transient is to blame for resolution decay and loss of lock. In Fig. 1 we see that most of the transient has decayed 600 ns after the feedback and address switch, but a small transient persists to about 1 μs. As t_{SET} is decreased toward the length of the transient, V_{ER} does not reach a value reflecting the true TES current before being sampled and the resolution degrades (henceforth, the t_{SET} effect). For $t_{SET} \leq 0.56$ μs, the loop unlocks.

Based on the data from the two-pixel experiment, we optimize the timing parameters for four multiplexed pixels, choosing $t_{SET} = 1.02$ μs, which, given $t_{SAM} = 0.04$ μs and $N_{MUX} = 4$, yields $t_{FR} = 4.24\mu$s. Fig. 2 shows that the t_{FR} and t_{SET} effects each should contribute a resolution degradation of about 0.15 eV from the nominal 6.5 eV, so we should expect about 6.8 ± 0.08 eV resolution from four multiplexed pixels. The measured spectra,
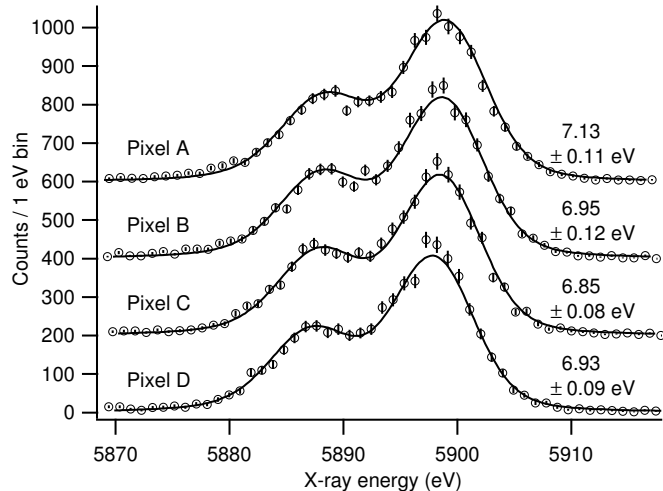
FIG. 3: Histogrammed pulse-energy spectra with overlaid fits to the Mn $K\alpha$ complex for four multiplexed TES pixels. The spectra are offset vertically by 200 counts/eV. Non-multiplexed resolution is 6.5 eV (FWHM); the slight degradation to an average resolution of 6.94 ± 0.05 eV is well explained by the t_{FR} and t_{SET} effects.

shown in Fig. 3, yield an average resolution of 6.94 ± 0.05 eV.

The present multiplexer system can stay locked on a maximum of eleven sensors, and can read out only six with 1 eV or less degradation of resolution. Fortunately, a set of straightforward improvements could ease the constraints on both t_{FR} and t_{SET}. The t_{FR} effect, most pronounced during fast-changing signals on a pulse rise, could be alleviated by adding inductance to the TES bias circuit in order to slow τ_{rise}. If we were to double τ_{rise}, we could double the value of t_{FR} at which signal degradation occurs and still keep the TESs well within the stability criterion[11] of $\tau_{fall}/\tau_{rise} > 3 + 2\sqrt{2}$.

If the switching transient (see Fig. 1) were shortened, the multiplexer could be run faster. The transient could be shortened by 110 nsec by improving the digital-feedback firmware to compensate for signal-propagation delay through the cryostat and coaxial cables. The remainder of the switching transient is governed by the open-loop system bandwidth, f_{OL}. The shape of the transient stems from the decaying signal from the turned-off pixel having a different time constant from the settling signal of the turned-on pixel, as $\tau_{L/R}$ for the first-stage-SQUID bias circuit is higher with the SQUID off than on. The smallest measured f_{OL} is 1.1 MHz ($\tau_{OL} = 145$ ns), a value dominated by the dynamic resistance of the second-stage SQUID in series with a high-inductance, superconducting-twisted-pair cable linking
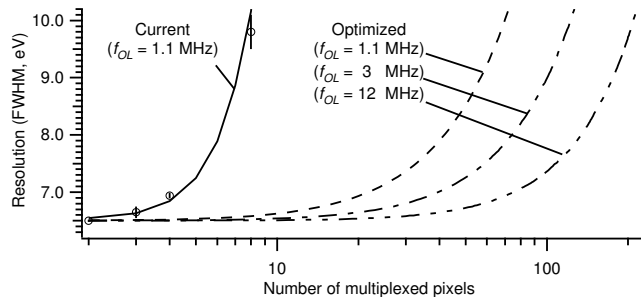
6

FIG. 4: Energy resolution vs. number of multiplexed pixels for the current multiplexer (solid) and various modifications (dashed). The curves show the predicted resolution based on effects measured in Fig. 2 and also on SQUID noise aliasing. Data (circles) are for $N_{MUX} = 2, 3, 4$, and 8 (the data point for 8 pixels uses four blank pixel periods, and thus simulates the switching and timing of eight multiplexed pixels with the four available sensors). The three dashed curves are predictions for various open-loop system bandwidths (f_{OL}), and also include twice the pulse τ_{rise}, SQUID amplifier noise half that in the current multiplexer chip, data-acquisition firmware correction for propagation delays, and optimized coupling between the TES and first-stage SQUID. More involved upgrades, including transmission-line optimization of the couplings among the cold amplifier stages and a substantial upgrade in the clock rate of the digital-feedback electronics, could allow f_{OL} of up to 100 MHz.

the 62 mK electronics to the 4 K, series-array-SQUID amplifier. After removing the 110 ns due to the propagation delay described above, the multiplexer locks while $t_{SET} > 3.1\tau_{OL}$, but degrades resolution if $t_{SET} < 6.5\tau_{OL}$ (see Fig. 2). We believe that the $f_{OL} = 3$ MHz measured in a 4 K demonstration of this multiplexer[2] could be recovered by replacing the superconducting twisted-pair cable with a low-inductance, coplanar, Nb-on-polyimide interconnect presently under development at NIST. Furthermore, other straightforward upgrades, such as increasing the dynamic resistance of the second-stage SQUID and removing inductance from the first-stage-SQUID bias loop, should increase f_{OL} to at least 12 MHz in the next-generation multiplexer, allowing t_{SET} of 80 ns or shorter. In addition, we estimate that with a significant upgrade of the room-temperature feedback electronics, it will be possible to increase f_{OL} to 100 MHz for 32 pixels with flux noise (referred to the first stage SQUID) as low as 0.1 $\mu\Phi_0/\sqrt{\text{Hz}}$.

The final of the straightforward improvements to the system would be to optimize the

mutual inductance of the TES coupling to the first-stage SQUID. Lower coupling would reduce the TES signal seen by the multiplexer, further alleviating the t_{FR} effect. However, lower coupling would also decrease the margin between the TES noise and SQUID noise. Aliased SQUID noise grows with increasing f_{OL}. We have recently tested a new first-stage SQUID design with lower noise (0.25 vs. 0.50 $\mu\Phi_0/\sqrt{\text{Hz}}$ in the current multiplexer chip), allowing lower TES coupling due to the increased noise margin. Fig. 4 shows the predicted effects of several upgrades on resolution and the number of pixels that can be multiplexed.

To conclude, we have tested an array of four time-division-multiplexed X-ray microcalorimeters, achieving a resolution of 6.94 ± 0.05 eV, which represents a degradation due to the multiplexer of only 0.44 eV. After modest and achievable system improvements, we predict the ability to multiplex a linear array of 32 of these pixels, and thus a square, kilopixel array, with a degradation in resolution of only 0.1 eV. In addition, we estimate that more substantial upgrades to f_{OL} should allow, within this time-division-multiplexer architecture, the instrumentation of kilopixel arrays with 100 μs response times and 2 eV energy resolution at 6 keV.

---

[1] J. A. Chervenak et al., Appl. Phys. Lett. **74**, 4043 (1999).

[2] P. A. J. de Korte et al., Rev. Sci. Instrum. **74**, 3807 (2003).

[3] C. D. Reintsema et al., Rev. Sci. Instrum. **74**, 4500 (2003).

[4] J. Yoon et al., Appl. Phys. Lett. **78**, 371 (2001).

[5] M. F. Cunningham et al., Appl. Phys. Lett. **81**, 159 (2002).

[6] J. van den Kuur et al., Appl. Phys. Lett. **81**, 4467 (2002).

[7] K. D. Irwin et al., Nucl. Instrum. Methods Phys. Res., Sect. A **520**, 544 (2004).

[8] M. E. Huber et al., IEEE Trans. Appl. Supercond. **11**, 4048 (2001).

[9] A. E. Szymkowiak et al., J. Low Temp. Phys. **93**, 281 (1993).

[10] G. Holzer et al., Phys. Rev. A **56**, 4554 (1997).

[11] K. D. Irwin et al., J. Appl. Phys. **83**, 3978 (1998).